Nanostructured polymetallaynes of controlled length: Synthesis and characterization of oligomers and polymers from 1,1′-Bis-(ethynyl)4, 4′-biphenyl bridging Pt(II) or Pd(II) center...

ARTICLE *in* JOURNAL OF POLYMER SCIENCE PART A POLYMER CHEMISTRY · AUGUST 2007

Impact Factor: 3.11 · DOI: 10.1002/pola.22081

4 AUTHORS, INCLUDING:

Ilaria Fratoddi
Sapienza University of Rome
92 PUBLICATIONS **961** CITATIONS
SEE PROFILE

Maria Vittoria Russo
Sapienza University of Rome
210 PUBLICATIONS **2,967** CITATIONS
SEE PROFILE

Nanostructured Polymetallaynes of Controlled Length: Synthesis and Characterization of Oligomers and Polymers from 1,1′-Bis-(ethynyl)4,4′-biphenyl Bridging Pt(II) or Pd(II) Centers

ILARIA FRATODDI,[1] CHIARA BATTOCCHIO,[2] ALESSANDRA L. GROIA,[1] MARIA V. RUSSO[1]

[1]Department of Chemistry, University ''La Sapienza'' of Rome, P.le A. Moro 5, Box 34 Roma 62, Rome, Italy

[2]Department of Physics, University ''Roma Tre'', Via della Vasca Navale 85, 00146 Rome, Italy

Received 29 January 2007; accepted 7 March 2007
DOI: 10.1002/pola.22081
Published online in Wiley InterScience (www.interscience.wiley.com).

ABSTRACT: The reactivity of square planar palladium(II) and platinum(II) complexes in trans or cis configuration, namely *trans* or *cis*-[dichlorobis(tributylphosphine)platinum(II)] and *trans*-[dichlorobis(tributylphosphine)palladium(II)] with 1,1′-bis(ethynyl) 4,4′-biphenyl, DEBP, leading to π-conjugated organometallic oligomeric and polymeric metallaynes, was investigated by a systematic variation of the reaction conditions. The formation of polymers and oligomers with defined chain length $[-M(PBu_3)_2(C\equiv C-C_6H_4-C_6H_4-C\equiv C-)]_n$ (n = 3–10 for the oligomers, n = 20–50 for the polymers) depends on the configuration of the precursor Pt(II) and Pd(II) complexes, the presence/absence of the catalyst CuI, and the reaction time. A series of model reactions monitored by XPS, GPC, and NMR ^{31}P spectroscopy showed the route to modulate the chain growth. As expected, the nature of the transition metal (Pt or Pd) and the molecular weight of the polymers markedly influence the photophysical characteristics of the polymetallaynes, such as optical absorption and emission behavior. Polymetallaynes with nanostructured morphology could be obtained by a simple casting procedure of polymer solutions. © 2007 Wiley Periodicals, Inc. J Polym Sci Part A: Polym Chem 45: 3311–3329, 2007

Keywords: conjugated polymers; morphology; organometallic polymers; polymetallaynes; transition metal chemistry

INTRODUCTION

Great attention has been paid by the scientific community to the synthesis and characterization of polymeric conjugated systems containing transition metal centers σ- or π-bonded to the organic main chain.[1,2] The study of chemicophysical, optical, and electrochemical properties of organometallic polymers may be oriented to the design of supramolecular systems suitable for technological applications such as LED or sensor construction.[3] These materials may combine the easy processing and peculiar mechanical properties of polymers with the tailored electronic and optical properties of functional organic molecules.[4,5] The modulation of the electronic properties of conjugated macromolecules may find a useful tool by the introduction of transition metals into conjugated polymers. In this way, it is possible to tailor both components (metal and spacer) of these systems and exploit different

Correspondence to: Dr. I. Fratoddi (E-mail: ilaria.fratoddi@uniroma1.it)

Journal of Polymer Science: Part A: Polymer Chemistry, Vol. 45, 3311–3329 (2007)

properties, for example, solubility, processability, charge-transfer-, redox-, and energy transfer processes.

Organometallic polymers can be obtained from blends of metal complexes and conjugated polymers,[6] as well as by incorporation of metal centers into polymers through coordinative bonds. In this case, the metal atoms may be coordinated to the polymer backbone or to side groups.[7] Since the pioneering work of leading research groups[8,9] on the synthesis and optoelectronic properties of Pt-containing polymetallaynes, the research devoted to this class of materials found a dramatic extension. In fact, the chemistry of dichloro-bisphosphine Pt complexes in the presence of diacetylenes is a very versatile tool for the achievement of complicated organometallic macromolecules. For example, dendritic networks,[10] oligomeric Pt-tetraethynylethene molecular scaffoldings,[11] and long chain linear polymetallaynes with photoluminescence and photoconducting properties[12] have been recently reported, and studies on the synthesis and linear optical properties of Pt(II) fluorine-bridged polymetallaynes (and related model complexes) have elucidated the tuning of the optical energy band gap on the length of the bridging acetylenic moiety,[13] as well as nonlinear optical behavior of related polyplatinaynes used in NLO optical limiting applications.[14]

Moreover, polymetallaynes can be considered as low-dimensional materials, and in proper conditions, can be deposited as nanostructured fibrils likewise to nanowires or nanocolumns with anisotropic properties, fundamental in nanodevice applications. It has been suggested that semiconductor wires thinner than 100 nm in diameter can be used to develop 1D quantum-wire high-speed field effect transistors and light-emitting devices with extremely low power consumption.[15]

Quite recently, our research focused on metallayne oligomers[16] as structural models for the related polymers and as effective materials for applications, because of the relatively easier access with respect to the corresponding polymers. The reactivity of the α-ω conjugated dialkyne, 1,1′-bis(ethynyl)4,4′-biphenyl (H—C≡C—C_6H_4—C_6H_4—C≡C—H, DEBP) for the synthesis of organometallic complexes and polymers has been investigated under different aspects. Mononuclear and binuclear Pt(II) model complexes containing the DEBP spacer were synthesized,[17] and their structure compared with that of related organic molecules to evaluate the role of the metal center on the π-delocalization of the organic spacer.[18]

The oxidative and catalytic polymerization of DEBP gave evidence of the formation of a *rigid-rod* poly(ethynylaromatic) polymer,[19] stable up to 300 °C. Organometallic polymers of type —[M—$(PBu_3)_2$—C≡C—C_6H_4—C_6H_4—C≡C—]$_n$— with M = Pt(II) and Pd(II), namely Pt-DEBP and Pd-DEBP, were already synthesized and used as membranes in surface acoustic wave sensors,[20] showing high sensitivity toward relative humidity and sulfur-containing organic vapors.[21] *cis*-Platinum(II) ethynyl complexes and polymers based on bidentate phosphines and DEBP as organic spacer were recently reported,[22,23] and the evolution of the lowest singlet and triplet excited states in Pt(II), Au(I), or Hg(I) containing polymetallacetylenes was correlated with the presence of heavy metals that enable efficient intersystem crossing from S_1 to T_1 state.[24] Recent studies on sensors based on analogue polymetallaynes showed a higher sensitivity toward low relative humidity percentages when nanostructured membranes were employed.[25–27]

Owing to the interest of these materials for applications in electronic devices, careful solid state characterizations of the polymeric membranes were performed. Evidences of molecular orientation on different substrates of the polymeric materials were studied by means of near-edge X-ray absorption spectra spectroscopy. Polymeric chains resulted in orientation at a tilt angle of about 40° with respect to the surface normal[28] and successive extended X-ray absorption structure spectroscopy studies on a monolayer of Pd-DEBP polymer deposited on a chromium substrate allowed to determine the bond lengths between Pd and its neighbors as well as the C—C distances in the linear chain.[29]

We describe here the systematic study of the reactivity of the α-ω conjugated dialkyne DEBP with *cis* and *trans*-[$Pt(PBu_3)_3Cl_2$] and *trans*-[$Pd(PBu_3)_3Cl_2$]. The careful investigation of the dehydrohalogenation reaction conditions between the organic spacer and the metal complexes gave rise to the formation of either polymetallaynes and of oligomers of definite chain lengths. Polymers and oligomers of type: [—[M$(PBu_3)_2$—C≡C—C_6H_4—C_6H_4—C≡C—]$_n$—, where M = Pt or Pd, n = number of metal units, were obtained, and their optical properties as a function of their chain length were investigated. The

DOI 10.1002/pola

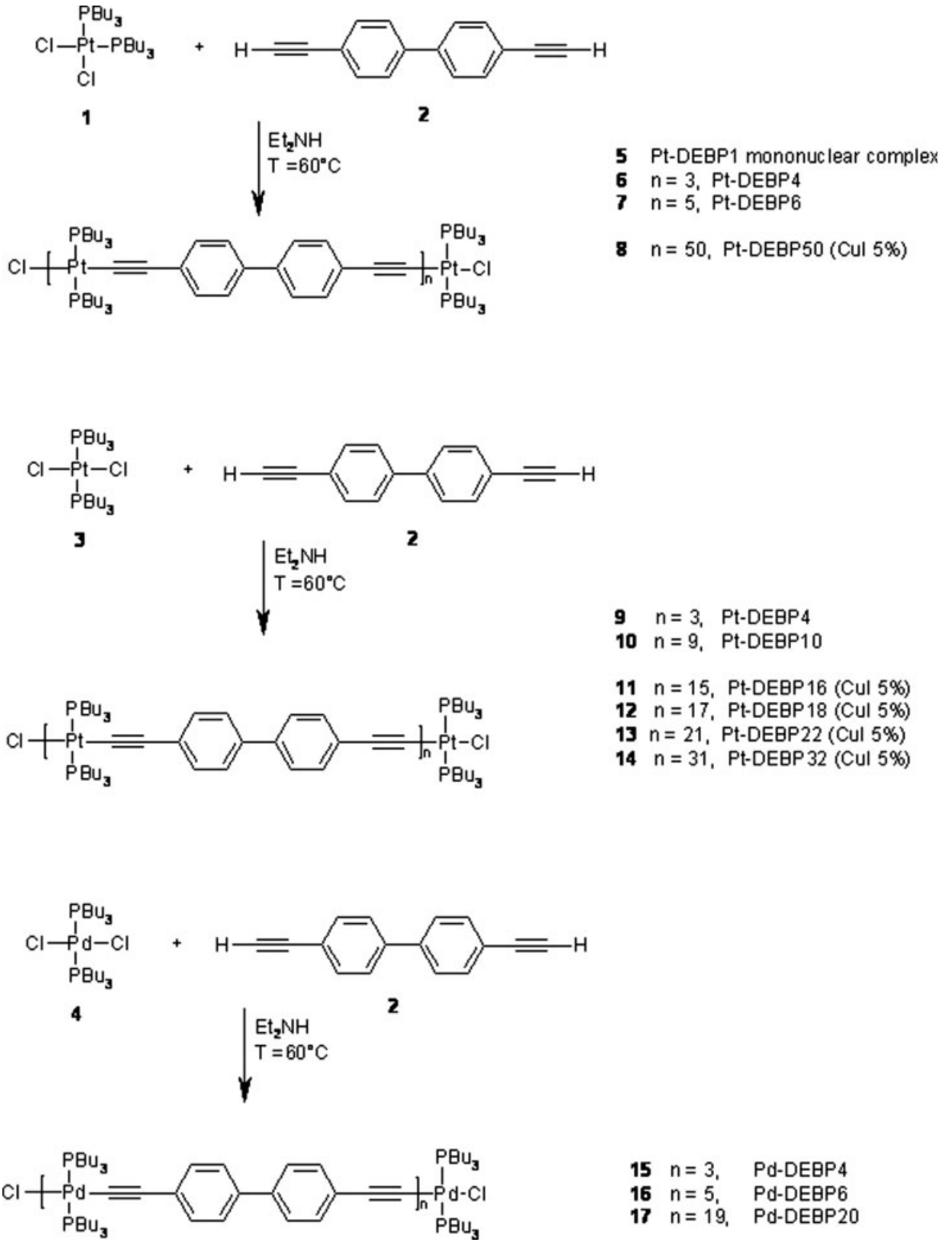

Figure 1. Molecular structures for Pt(II) and Pd(II) polymetallaynes.

molecular structures are depicted in Figure 1, and the main characterizations and molecular formulas are collected in Table 1.

Rigid-rod π-conjugated transition metal oligomers constitute a potentially new class of molecular wires. There have been several studies on

Table 1. Reaction Conditions for the Preparation of Pt(II) and Pd(II) Oligomers and Polymers (Solvent Diethylamine, Temperature $T = 60$ °C)

Precursor Complex	Sample	CuI (%)	Yield (%)	Reaction Time (h)	UV–Vis $CHCl_3$, $-\lambda_{ass}$[a] (nm)	^{31}P NMR, $CDCl_3$[b] (ppm)		Elemental Analyses	
						Internal	Terminal	C (%)	H (%)
1	**6** Pt-DEBP4	–	85	4	304.0; 360.0	3.77 (2356)[c]	7.54 (2374)	57.03 [56.33][d]	7.83 [7.88]
	7 Pt-DEBP6	–	75	24	302.6; 368.0	3.77 (2356)	7.52 (2374)	58.26 [57.60]	7.90 [7.86]
	8 Pt-DEBP50	5	92	24	303.8; 373.2	3.70 (2356)	7.52 (2374)	59.86 [60.06]	7.73 [7.81]
3	**9** Pt-DEBP4	–	94	4	304.0; 360.0	3.72 (2360)	7.52 (2371)	56.58 [56.33]	7.92 [7.88]
	10 Pt-DEBP10	–	94	24	365.2	3.72 (2360)	7.52 (2371)	58.98 [58.60]	7.56 [7.84]
	11 Pt-DEBP16	5	78	8	370.6	3.70 (2358)	7.51 (2370)	59.27 [60.06]	8.04 [7.81]
	12 Pt-DEBP18	5	92	10	371.6	3.71 (2358)	7.51 (2371)	58.89 [60.06]	8.17 [7.81]
	13 Pt-DEBP22	5	76	12	373.0	3.69 (2358)	7.50 (2370)	59.34 [60.06]	7.99 [7.81]
	14 Pt-DEBP32	5	84	24	373.0	3.72 (2358)	7.52 (2371)	59.20 [60.06]	8.09 [7.81]
4	**15** Pd-DEBP4	–	82	4	343.6	11.32	10.50	64.99 [63.68]	8.95 [8.91]
	16 Pd-DEBP6	–	60	24	343.5	11.26	10.48	65.56 [65.01]	8.73 [8.86]
	17 Pd-DEBP20	–	78	8	343.2	11.29	10.47	65.87 [67.54]	8.87 [8.79]

[a] λ_{ass} (maximum absorption wavelength).
[b] Referred to H_3PO_4 85%.
[c] Values in parentheses indicate J in Hertz.
[d] Values in square brackets indicate theoretical elemental analyses in percentages.

electron transfer involving organic oligomers with thiol-based end groups, which are fundamental for the formation of self-assembled monolayers or covalent connections between proximate gold electrodes.[30,31] On the basis of recent theoretical studies by Oleynik et al.[32] concerning molecular electronic studies of thiophene-based diblock oligomers, a molecular diode behavior has been established. The driving force for this research is the expectation of faster electronic systems through the miniaturization of microelectronic components to the scale of atoms and molecules.[33,34] In this framework, the deposition modes suitable for the formation of Pt-DEBP and Pd-DEBP nanostructures with different morphologies have also been developed in view of improved applications of these materials in sensor and optical devices. It is noteworthy that the morphological features of polymetallaynes are so far little studied. The morphology of Pt-DEBP and Pd-DEBP films was detected by means of SEM measurements, and the factors affecting the growth of molecular self-assembling was assessed.

EXPERIMENTAL

Instrumentation

FTIR spectra were recorded as nujol mulls or as films deposited from $CHCl_3$ solutions by using CsI cells, on a PerkinElmer 1700× Fourier transform spectrometer. ^1H, ^{31}P NMR spectra were recorded on a Bruker AC 300P spectrometer at 300 and 121 MHz, respectively, in appropriate solvents ($CDCl_3$); the chemical shifts (ppm) were referenced to TMS for ^1H NMR assigning the residual ^1H impurity signal in the solvent at 7.24 ppm ($CDCl_3$). ^{31}P NMR chemical shifts are relative to H_3PO_4 (85%). UV–vis spectra were recorded on a PerkinElmer λ-16 instrument. Photoluminescence spectra were performed on a PerkinElmer LS 50 Fluorescence Spectrometer. All measurements were performed at room temperature using quantitative solutions of the oligomers in $CHCl_3$. The molar extinction coefficient ε_o (with respect to the repeating unit) and the relative quantum yield η were also determined. We adopted as the standard a solution of coumarine in ethanol (c = 0.0028 g/L), with a quantum yield equal to 51%, calculated by comparison with a rhodamine 6G solution (c = 0.016 g/L, η = 90%). Quantitative solutions of coumarine and of oligomers were prepared on purpose,[35] with the same absorbance at the excitation wavelength λ_{max} = 350 nm. The relative quantum yields were calculated from the measurements of the emission intensities of the sample and of the standard, considering the relationship: $\eta_{sample} = (I_{sample}/I_{standard}) \times \eta_{standard}$. All the data were corrected by taking into account the photomultiplier efficiency of the fluorescence spectrometer.

Thermogravimetric analysis (TGA) and differential scanning calorimetry (DSC) were performed with the PerkinElmer TGA6 and PerkinElmer Pyris Diamond thermal analyzers, respectively, at a heating rate of 20 °C/min. Molecular weights were determined by gel permeation chromatography (GPC) on a PerkinElmer instrument equipped with a PL-gel column and UV detector. Measurements were performed in $CHCl_3$ (HPLC grade), using monodisperse polystyrene standards at 25 °C, at a flow rate of 1 mL/min. Elemental analyses were performed at the Department of Chemistry, University of Rome "La Sapienza."

XPS spectra were obtained using a custom-designed spectrometer. A nonmonochromatized Mg Kα X-rays source (1253.6 eV) was used, and the pressure in the instrument was maintained at 1×10^{-9} Torr throughout the analysis. The experimental apparatus consists of an analysis chamber and a preparation chamber separated by a gate valve. An electrostatic hemispherical analyser (radius 150 mm) operating in the fixed analyser transmission mode and a 16-channel detector were used. The film samples were prepared by dissolving our materials in $CHCl_3$ and spinning the solutions onto polished stainless steel substrates. The samples showed good stability during the XPS analysis, preserving the same spectral features and chemical composition. The experimental energy resolution was 1 eV on the Au $4f_{7/2}$ component. The resolving power $\Delta E/E$ was 0.01. Binding energies (BE) were corrected by adjusting the position of the C1s peak to 285.0 eV in those samples containing mainly aliphatic carbons and to 284.7 eV in those containing more aromatic carbon atoms, in agreement with literature data.[36] The C1s, Pd3d, Pt4f, P2p, and Cl2p spectra were deconvoluted into their individual peaks using the *peak fit* curve fitting program for PC. Quantitative evaluation of the atomic ratios was obtained by analysis of the XPS signal intensity, employing Scofield's atomic cross section values[37] and experimentally determined sensitivity factors.

Synthesis: General Preparation of Polymetallaynes and Oligomers

All reactions were performed under an inert argon atmosphere. Solvents were dried on Na_2SO_4 before use. All chemicals, unless otherwise stated, were obtained from commercial sources and used as received. The compound **4**, DEBP was prepared according to literature methods.[38] Platinum and palladium complexes $[MCl_2(PBu_3)_2]$, with M = Pt or Pd, that is *cis*-[dichlorobis(tributylphosphine)platinum(II)], *trans*-[dichlorobis(tributylphosphine)platinum(II)], and *trans*-[dichlorobis(tributylphosphine)palladium(II)], were prepared by reported methods.[39] Preparative thin-layer chromatography separation was performed on 0.7-mm silica plates (Merck Kieselgel 60 GF254) and chromatographic separations were obtained with 70–230 mesh alumine (Merck), by using *n*-hexane/dichlorometane mixtures. Thin films of Pt-DEBP or Pd-DEBP polymers were obtained by casting $CHCl_3$ or toluene solutions (1 mg/mL) at room temperature on glass or gold substrates, controlling the evaporation rate of the polymeric solution.

Typical Procedure for the Synthesis

DEBP (0.8 mmol) and an equimolar amount of the Pt(II) or Pd(II) complexes $[M(PBu_3)_2Cl_2]$ were added in the reaction flask in the presence of argon-bubbled diethylamine as solvent and base (30 mL). The reactions were allowed to react for different times at 60 °C. Ammonium salts were then removed by filtration and the residual dark brown solution reduced in volume with a rotating evaporator. The reactions were carried out with or without CuI as catalyst (5% in mol), as indicated in the Table 1. The products were then extracted with CH_2Cl_2/H_2O and a pale yellow powder (M-DEBP*n*) was formed by adding methanol and then filtered off. Oligomers with different chain length could be obtained by chromatographic separation on silica (*n*-hexane/dichlorometane mixture from 1/9 to 3/7 ratio) of crude reaction products, from reactions carried out with different times, as reported in Table 1.

Characterization of the Reaction Products

5, Pt-DEBP1: ^{1}H NMR ($CDCl_3$, ppm): 7.44 (d, 4H, Ar—*H*), 7.32 (d, 4H, Ar—*H*), 7.54 (s, 4H, Ar—*H*), 2.02 (m, 12H, P—C*H*$_2$—), 1.59 (m, 12H, P—CH_2—C*H*$_2$—), 1.46 (q, 12H, P—CH_2—CH_2—C*H*$_2$—), 0.93 (t, 18H, —CH_3 J = 9.00 Hz); ^{31}P NMR ($CDCl_3$, ppm (J^{195}Pt-^{31}P) Hz) 7.54 (2374).

6, Pt-DEBP4: IR (film, cm^{-1}) ν(C≡C): 2099; 2932, 2972, 2872,1602, 1489, 1463, 1410, 1379, 1214, 1094, 904, 823, 757, 722; UV ($CHCl_3$): 304.0; 360.0 nm; ^{1}H NMR ($CDCl_3$, ppm): 7.44 (d, 4H, Ar—*H*), 7.32 (d, 4H, Ar—*H*), 7.54 (s, 4*H*, Ar—H), 2.16 (m, 12H, P—C*H*$_2$—), 2.12 (m, 12H, P—C*H*$_2$—), 1.59 (m, 12H, P—CH_2—C*H*$_2$—),1.46 (q, 12H, P—CH_2—CH_2—C*H*$_2$—), 0.93 (t, 18H, —CH_3 J = 9.00 Hz); ^{31}P NMR ($CDCl_3$, ppm (J^{195}Pt-^{31}P) Hz): 3.77 (2356), 7.54 (2374), integral intensity ratio 1:1; ELEM. ANAL. (%), found (calculated for the tetranuclear oligomer $C_{144}H_{240}Cl_2P_8Pt_4$): C = 57.03 (56.33); H = 7.83 (7.88).

7, Pt-DEBP6: IR (film, cm^{-1}) ν(C≡C): 2099; 2932, 2972, 2872, 2483, 2099, 1602, 1485, 1464, 1262, 1093, 823, 720, 453, 396, 316; UV ($CHCl_3$): 302.6; 368.0 nm; ^{1}H NMR ($CDCl_3$, ppm): 7.43 (d, 4H, Ar—*H*), 7.29 (d, 4H, Ar—*H*), 7.54 (s, 4*H*, Ar—H), 2.17 (m, 12H, P—C*H*$_2$—), 2.01 (m, 12H, P—C*H*$_2$—), 1.61 (m, 12H, P—CH_2—C*H*$_2$—),1.44 (q, 12H, P—CH_2—CH_2—C*H*$_2$—), 0.93 (t, 18H, —CH_3 J = 9.00 Hz); ^{31}P NMR ($CDCl_3$, ppm (J^{195}Pt-^{31}P) Hz): 3.77 (2356), 7.52 (2374), integral intensity ratio 2:1; ELEM. ANAL. (%), found (calculated for the hexanuclear oligomer $C_{224}H_{364}Cl_2P_{12}Pt_6$): C = 58.26 (57.60); H = 7.90 (7.86).

8, Pt-DEBP50: IR (film, cm^{-1}) ν(C≡C): 2096; 2932, 2972, 2872, 1602, 1486, 1464, 1378, 1212, 1094, 903, 822, 720, 462, 396; UV ($CHCl_3$): 303.8; 373.2 nm; ^{1}H NMR ($CDCl_3$, ppm): 7.43 (d, 4H, Ar—*H*), 7.29 (d, 4H, Ar—*H*), 7.52 (s, 4*H*, Ar—H), 2.13 (m, 12H, P—C*H*$_2$—), 1.59 (m, 12H, P—CH_2—C*H*$_2$—),1.43 (q, 12H, P—CH_2—CH_2—C*H*$_2$—), 0.92 (t, 18H, —CH_3 J = 9.00 Hz); ^{31}P NMR ($CDCl_3$, ppm (J^{195}Pt-^{31}P) Hz): 3.70 (2356), 7.52 (2374), integral intensity ratio 25:1; ELEM. ANAL. (%), found (calculated for the repeating unit $C_{40}H_{62}P_2Pt$): C = 59.86 (60.06); H = 7.73 (7.81).

9, Pt-DEBP4: IR (film, cm^{-1}) ν(C≡C): 2100; 2932, 2972, 2872, 1602, 1489, 1463, 1373, 1213, 1093, 1053, 971, 904, 822, 720, 450, 400, 364, 312, 280; UV ($CHCl_3$): 304.0; 360.0 nm; ^{1}H NMR ($CDCl_3$, ppm): 7.45 (d, 4H, Ar—*H*), 7.30 (d, 4H, Ar—*H*), 7.53 (s, 4*H*, Ar—H), 2.16 (m, 12H, P—C*H*$_2$—), 1.99 (m, 12H, P—C*H*$_2$—), 1.61 (m, 12H, P—CH_2—C*H*$_2$—),1.44 (q, 12H, P—CH_2—CH_2—C*H*$_2$—), 0.93 (t, 18H, —CH_3 J = 9.00 Hz); ^{31}P NMR ($CDCl_3$, ppm (J^{195}Pt-^{31}P) Hz): 3.72 (2360), 7.52 (2371), integral intensity ratio

1:1; ELEM. ANAL. (%), found (calculated for the tetranuclear oligomer $C_{144}H_{240}Cl_2P_8Pt_4$): C = 56.58 (56.33); H = 7.92 (7.88).

10, Pt-DEBP10: IR (film, cm^{-1}) ν(C≡C): 2099; 2955, 2972, 2871, 1602, 1486, 1464, 1379, 1212, 1093, 1053, 971, 904, 822, 720, 450, 400, 364, 312, 280; UV ($CHCl_3$): 365.2 nm; ^{1}H NMR ($CDCl_3$, ppm): 7.45 (d, 4H, Ar—*H*), 7.30 (d, 4H, Ar—*H*), 7.53 (s, 4*H*, Ar—H), 2.16 (m, 12H, P—CH_2—), 1.99 (m, 12H, P—CH_2—), 1.61 (m, 12H, P—CH_2—CH_2—),1.44 (q, 12H, P—CH_2—CH_2—CH_2—), 0.93 (t, 18H, —CH_3 J = 9.00 Hz); ^{31}P NMR ($CDCl_3$, ppm (J^{195}Pt-^{31}P) Hz): 3.72 (2360), 7.52 (2371), integral intensity ratio 4:1; ELEM. ANAL. (%), found (calculated for the decanuclear oligomer $C_{384}H_{612}Cl_2P_{20}Pt_{10}$): C = 58.98 (58.60); H = 7.56 (7.84).

11, Pt-DEBP16: IR (film, cm^{-1}) ν(C≡C): 2097; 2932, 2870, 1602, 1485, 1461, 1263, 1092, 904, 821, 720, 540, 467, 450, 401, 393; UV ($CHCl_3$): 370.6 nm; ^{1}H NMR ($CDCl_3$, ppm): 7.46 (d, 4H, Ar—*H*), 7.30 (d, 4H, Ar—*H*), 7.56 (s, 4*H*, Ar—H), 2.12 (m, 12H, P—CH_2—), 2.01 (m, 12H, P—CH_2—), 1.61 (m, 12H, P—CH_2—CH_2—),1.46 (q, 12H, P—CH_2—CH_2—CH_2—), 0.94 (t, 18H, —CH_3 J = 9.00 Hz); ^{31}P NMR ($CDCl_3$, ppm (J^{195}Pt-^{31}P) Hz): 3.70 (2358), 7.51 (2371), integral intensity ratio 7:1; ELEM. ANAL. (%), found (calculated for the repeating unit $C_{40}H_{62}P_2Pt$): C = 59.27 (60.06); H = 8.04 (7.81).

12, Pt-DEBP18: IR (film, cm^{-1}) ν(C≡C): 2097; 2932, 2870, 1602, 1485, 1461, 1263, 1092, 904, 821, 720, 540, 467, 450, 401, 393; UV ($CHCl_3$): 371.6 nm; ^{1}H NMR ($CDCl_3$, ppm): 7.43 (d, 4H, Ar—*H*), 7.30 (d, 4H, Ar—*H*), 2.14 (m, 12H, P—CH_2—), 1.61 (m, 12H, P—CH_2—CH_2—), 1.41 (q, 12H, P—CH_2—CH_2—CH_2—), 0.92 (t, 18H, —CH_3 J = 9.00 Hz); ^{31}P NMR ($CDCl_3$, ppm (J^{195}Pt-^{31}P) Hz): 3.71 (2358), 7.51 (2371), integral intensity ratio 8:1; ELEM. ANAL. (%), found (calculated for the repeating unit $C_{40}H_{62}P_2Pt$): C = 58.89 (60.06); H = 8.17 (7.81).

13, Pt-DEBP22: IR (film, cm^{-1}) ν(C≡C): 2096; 2932, 2870, 1602, 1486, 1464, 1212, 1094, 903, 822, 720, 452, 390; 322, 280; UV ($CHCl_3$): 373.0 nm; ^{1}H NMR ($CDCl_3$, ppm): 7.43 (d, 4H, Ar—*H*), 7.29 (d, 4H, Ar—*H*), 2.13 (m, 12H, P—CH_2—), 1.60 (m, 12H, P—CH_2—CH_2—),1.43 (q, 12H, P—CH_2—CH_2—CH_2—), 0.92 (t, 18H, —CH_3 J = 9.00 Hz); ^{31}P NMR ($CDCl_3$, ppm (J^{195}Pt-^{31}P) Hz): 3.69 (2358), 7.50 (2371), integral intensity ratio 10:1; ELEM. ANAL. (%), found (calculated for the repeating unit $C_{40}H_{62}P_2Pt$): C = 59.34 (60.06); H = 7.99 (7.81).

14, Pt-DEBP32: IR (film, cm^{-1}) ν(C≡C): 2094; 2932, 2870, 1602, 1485, 1463, 1373, 1213, 1093, 971, 904, 720, 401, 393; UV ($CHCl_3$): 372.2 nm; ^{1}H NMR ($CDCl_3$, ppm): 7.44 (d, 4H, Ar—*H*), 7.29 (d, 4H, Ar—*H*), 2.15 (m, 12H, P—CH_2—), 1.62 (m, 12H, P—CH_2—CH_2—),1.45 (q, 12H, P—CH_2—CH_2—CH_2—), 0.93 (t, 18H, —CH_3 J = 9.00 Hz); ^{31}P NMR ($CDCl_3$, ppm (J^{195}Pt-^{31}P) Hz): 3.72 (2358), 7.52 (2371), integral intensity ratio 8:1; ELEM. ANAL. (%), found (calculated for the repeating unit $C_{40}H_{62}P_2Pt$): C = 59.20 (60.06); H = 8.09 (7.81).

15, Pd-DEBP4: IR (film, cm^{-1}) ν(C≡C): 2096; 2932, 2872, 1601, 1488, 1463, 1378, 1210, 1092, 903, 721, 443, 396; UV ($CHCl_3$): 343.6 nm; ^{1}H NMR ($CDCl_3$, ppm): 7.44 (d, 4H, Ar—*H*), 7.28 (d, 4H, Ar—*H*), 2.02 (m, 12H, P—CH_2—), 1.58 (m, 12H, P—CH_2—CH_2—),1.43 (q, 12H, P—CH_2—CH_2—CH_2—), 0.92 (t, 18H, —CH_3 J = 9.00 Hz); ^{31}P NMR ($CDCl_3$, ppm): 11.32, 10.50, integral intensity ratio 1:1; ELEM. ANAL. (%), found (calculated for the tetranuclear oligomer $C_{144}H_{240}Cl_2P_8Pd_4$): C = 64.99 (63.68); H = 8.95 (8.91).

16, Pd-DEBP6: IR (film, cm^{-1}) ν(C≡C): 2096; 2932, 2872, 1601, 1488, 1463, 1378, 1210, 1092, 903, 721, 443, 396; UV ($CHCl_3$): 343.5 nm; ^{1}H NMR ($CDCl_3$, ppm): 7.44 (d, 4H, Ar—*H*), 7.28 (d, 4H, Ar—*H*), 2.10 (m, 12H, P—CH_2—), 1.61 (m, 12H, P—CH_2—CH_2—),1.42 (q, 12H, P—CH_2—CH_2—CH_2—), 0.92 (t, 18H, —CH_3 J = 9.00 Hz); ^{31}P NMR ($CDCl_3$, ppm): 11.26, 10.48, integral intensity ratio 2:1; ELEM. ANAL. (%), found (calculated for the hexanuclear oligomer C_{224} H_{364} $Cl_2P_{12}Pt_6$): C = 65.56 (65.01); H = 8.73 (8.86).

17, Pd-DEBP20: IR (film, cm^{-1}) ν(C≡C): 2096; 2932, 2872, 1601, 1488, 1463, 1378, 1210, 1092, 903, 721, 443, 396; UV ($CHCl_3$): 352.6 nm; ^{1}H NMR ($CDCl_3$, ppm): 7.44 (d, 4H, Ar—*H*), 7.28 (d, 4H, Ar—*H*), 2.02 (m, 12H, P—CH_2—), 1.58 (m, 12H, P—CH_2—CH_2—),1.43 (q, 12H, P—CH_2—CH_2—CH_2—), 0.92 (t, 18H, —CH_3 J = 9.00 Hz); ^{31}P NMR ($CDCl_3$, ppm): 11.29, 10.47, integral intensity ratio 9:1; ELEM. ANAL. (%), found (calculated for the repeating unit $C_{40}H_{62}P_2Pd$): C = 65.56 (67.54); H = 8.87 (8.79).

RESULTS AND DISCUSSION

Synthesis and NMR Characterization of Pt-DEBP*n* Oligomers

Platinum oligomers and polymetallayne, Pt-DEBP*n*, were synthesized from *cis* or *trans*

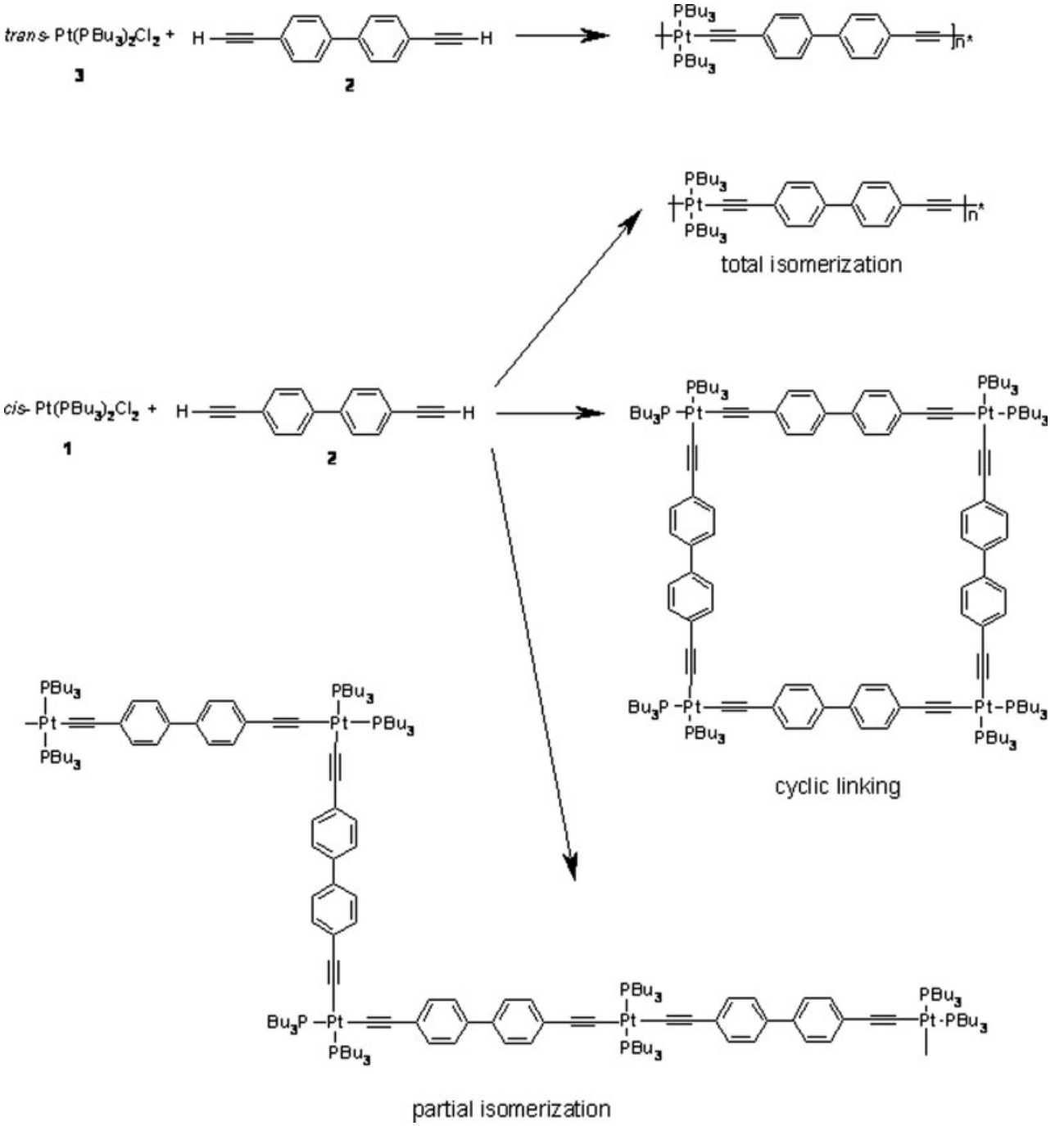

Figure 2. Proposed molecular structures of cis and trans polymetallaynes.

square planar bistributylphosphine-dichloride-platinum(II) complexes with the aim of verifying whether a given configuration around the transition metal is a prerequisite to obtain all trans polymetallaynes; alternatively, mixed cis/trans sequences may be obtained from a cis metal complex (*zigzag* structure) or even cyclic macrostructures,[40] as summarized in Figure 2. It is noteworthy that the isomerization reaction[41] of *cis*-[$Pt(PBu_3)_2Cl_2$] that leads to the thermodynamically stable complex trans isomer requires a long purification. The polycondensation reaction was carried out in dehydroalogenation conditions which, on the basis of the Hagihara method,[7] would require the use of precursor trans complexes.[42] An equimolar amount of

dichloride platinum complex was allowed to react with the terminal dialkyne DEBP[2] in diethylamine as solvent and base in different reaction conditions (Table 1). The role of the CuI catalyst was also considered, studying the reaction in the presence (5% mol) or absence of CuI. The intermolecular transfer mechanism of the alkynyl ligand from Cu(I) to Pt(II) is in fact well assessed for the formation of alkynyl complexex and molecules. CuI acts to make the cross coupling efficient by promoting selective and reversible transfer of the alkynyl ligand, and in the reaction mixture leads to several multinuclear $[Cu(C{\equiv}CR)L_n]_m$ structures.[43] The course of the polycondensation reactions was preliminary monitored with UV and ^{31}P NMR techniques, and then independent reactions were carried out for different times to achieve the oligomers with known chain length. The rationale that drew the experimental route will be hereafter described, considering first the NMR results that were the most indicative ones for the recognition of the geometry around the metal center and the number of repeating units in the oligomers; then, infrared, optical, thermal, electronic, and morphological characteristics will be reported and discussed.

Reactions of cis-*[Pt(PBu$_3$)$_2$Cl$_2$] with DEBP*

When the dehydrohalogenation reaction was carried out without the CuI catalyst at 60 °C in diethylamine, the formation of oligomers with chlorine terminal group was observed. A fast cis to trans isomerization of the precursor complex occurred; in fact, neither complexes nor oligomers with cis configuration were found, even in the first 30 min of reaction. The obtained materials showed a resonance at about 7.5 ppm in the ^{31}P NMR spectra, which was assigned to phosphorus centers bonded to terminal platinum units and a resonance at about 3.7 ppm due to metal centers internal in the chain, in agreement with literature data.[44] The absence of the resonance due to alkyne-H groups in the ^{1}H NMR spectra suggests that both terminal groups are Pt-Cl. The coupling constant $J(^{195}Pt\text{-}^{31}P)$ equal to 2360 Hz was in every case typical of a trans geometry around the metal.

^{31}P NMR spectra suggested the formation of a probable monochloride monoacetylide (*trans*) complex (**5**, Pt-DEBP1) identified in the reaction mixture at the first coupling stage (after 30 min of reaction) together with the just isomerized

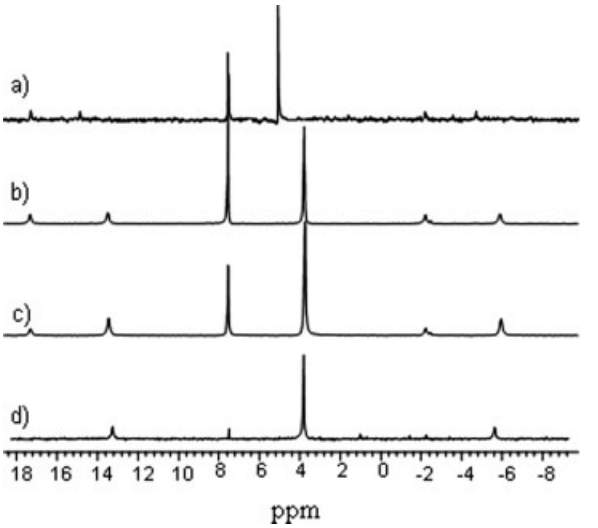

Figure 3. ^{31}P NMR spectra ($CDCl_3$): (a) complex 5, Pt-DEBP1; (b) tetranuclear oligomer 6, Pt-DEBP4; (c) hexanuclear oligomer 7, Pt-DEBP6; (d) polymetallayne 8, Pt-DEBP50.

trans-$[Pt(PBu_3)_3Cl_2]$ complex (5.05 ppm). The resonance at 7.54 ppm, shown in Figure 3(a), can be attributed to a monochloride complex in analogy with the resonances reported for homologue compounds.[45] The presence of product **5** was followed by the formation of different oligomers detected from ^{31}P NMR spectra recorded during the reaction course. In Figure 3(b,c), the spectra of oligomers obtained at different reaction times are reported.

In particular, with a reaction time of 4 h [Fig. 3(b)], a tetranuclear oligomer (**6**, Pt-DEBP4) was isolated after chromatographic separation, as the integral ratio 1:1 of the resonances at 7.54 and 3.77 ppm suggest. Considering a reaction time of 24 h, the polymerization reaction led to an oligomer with a number of platinum atoms equal to 6 (**7**, Pt-DEBP6) [Fig. 3(c), integral ratio of the resonances 1:2). It is noteworthy that, in the case of absence of the CuI catalyst, the polycondensation reaction easily leads to well-defined short-chain oligomers that can be considered as precursors of molecular wires by replacement of Cl terminals with thiol groups.

Previous studies demonstrated that, in slightly different reaction conditions, the dinuclear Pt complex *trans, trans*-$[ClPt(PBu_3)_2(-C{\equiv}C-C_6H_4-C_6H_4-C{\equiv}C-Pt(PBu_3)_2Cl]$ could be isolated.[17] XAS data analysis performed on the basis of the X-ray single crystal structure showed a partial conjugation within the molecule. The alkynyl units are essentially linear,

confirming the linearity of the whole molecule; the biphenyl moiety is strictly planar, and its mean plane disposes quite perpendicular to the coordination plane of the metal.

To study the influence of the CuI catalyst, the polycondensation reaction was then carried out in the presence of 5% of CuI catalyst at 60 °C. Polymeric compounds in trans configuration around the metal center were obtained in this case. ^{31}P NMR spectrum is reported in line d of Figure 3 for compound **8**, Pt-DEBP50; the two signals at 7.52 and 3.70 ppm, terminal and internal units, respectively, and integral ratio equal to 1:25 show a coupling constant of about 2300 Hz typical of trans configuration.

The ^{1}H NMR spectra of compounds **5–7** reported in Figure 4(a–c) further support the assessment of the oligomeric structure of these products. The observed resonances at 0.9, 1.5, 1.6, 2.0, and 2.2 ppm are due to the alkyls of the butyl phosphine ligand, whereas the signals downfield at 7.5, 7.4, and 7.3 ppm are due to the aromatic protons of the organic spacer DEBP. By carefully observing the resonances at 2.2 and 2.0 ppm, we observed that these signals derive from CH_2 directly bonded to P atom and that this CH_2 moiety resonance was strongly affected by the terminal or internal position of the metal center and appeared to split into two components. By comparing ^{31}P and ^{1}H spectra, a correlation can be achieved. Terminal and internal $Pt(PBu_3)_2$ moieties that give rise to the two ^{31}P signals at 7.5 and 3.7 ppm, respectively, can be used to attribute the ^{1}H NMR split signals found at 2.0 and 2.2 ppm, respectively. In fact, the integral ratio of the ^{31}P peaks due to terminal and internal moieties corresponds to the integral ratio of the ^{1}H NMR split resonances. In particular, for the tetranuclear compound **6**, Pt-DEBP4, the integral ratio of the signals at 2.16 and 2.04 ppm [Fig. 4(b)] is equal to 1:1, whereas for the hexanuclear compound **7**, Pt-DEBP6 [Fig. 4(c)], this ratio becomes 1:2. By this way, from the ^{1}H NMR study, a terminal group analysis is achieved, and an estimation of the chain length of the oligomers can be assessed. ^{1}H NMR (line d of Fig. 4) also supports the proposed structure for polymer **8**, Pt-DEBP50, showing a broad signal centered at 2.13 ppm, being absent for the component due to the terminal groups.

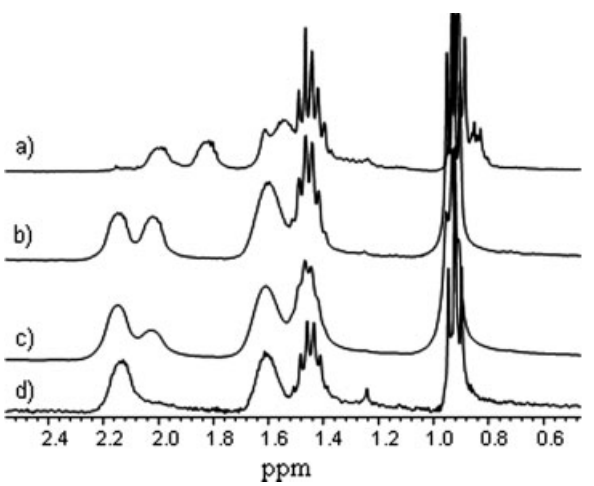

Figure 4. ^{1}H NMR spectra ($CDCl_3$): (a) complex 5, Pt-DEBP1; (b) tetranuclear oligomer 6, Pt-DEBP4; (c) hexanuclear oligomer 7, Pt-DEBP6; (d) polymetallayne 8, Pt-DEBP50.

Reactions of trans-*[Pt(PBu$_3$)$_2$Cl$_2$] with DEBP*

The polymerization reactions carried out starting from *trans*-[$Pt(PBu_3)_2Cl_2$], complex **3**, in the absence of CuI catalyst led to oligomeric materials with a number of repeating units in the range of 4–10 depending on the reaction time. The ^{31}P NMR spectra allowed to define the configuration around the metal center and the chain length from the relative intensities of the resonances at 3.72 and 7.52 ppm due to internal and external $Pt(PBu_3)_2$ moieties, respectively, with a coupling constant of 2360 and 2370 Hz typical of trans configuration. ^{1}H NMR spectra confirmed the chemical structures of the reaction products, with the same resonances assigned in the previous section. In particular with a reaction time of 4 h, the four units oligomer **9**, Pt-DEBP4, was isolated, whereas for 24-h reaction time an oligomer mainly constituted by 10 units, compound **10**, Pt-DEBP10 was obtained.

The polymerization reaction carried out in the presence of CuI (5%) produced the expected compounds with a chain length in the range of 16–32 repeating units. Performing the reaction for 8 h, an oligomer with about 16 metal centers was isolated after chromatographic separation. By increasing the reaction time up to 10, 12, and 24 h, oligomers/polymers mainly composed by 18, 22, and 32 units can be obtained (Table 1). It can be observed that in the presence of CuI and of the precursor complex **3**, the reaction goes straightforward to the formation of higher molecular weight oligomers.

Table 2. GPC Experimental Results ($CHCl_3$, $T = 30$ °C, Polystirene Standards) and IR Stretching Mode for C≡C Moiety

	Sample	M_w[a] (g mol^{-1})	M_n[b] (g mol^{-1})	MWD[c]	nM_w[d]	nM_n[e]	n[f]	MW[f] (g mol^{-1})	IR ν (C≡C) (cm^{-1})
6	Pt-DEBP4	3,800	2,500	1.52	5	3	4	3,070	2,099
7	Pt-DEBP6	8,600	4,600	1.87	11	6	6	4,670	2,099
8	Pt-DEBP50	42,000	13,000	3.23	52	16	50	40,000	2,096
9	Pt-DEBP4	4,300	2,600	1.65	5	3	4	3,070	2,100
10	Pt-DEBP10	10,000	4,800	2.10	12	6	10	7,870	2,099
11	Pt-DEBP16	11,200	5,600	2.00	14	7	16	12,670	2,097
12	Pt-DEBP18	13,000	4,600	2.82	16	6	18	13,470	2,097
13	Pt-DEBP22	16,000	10,000	1.60	20	12	22	17,470	2,096
14	Pt-DEBP32	24,000	12,000	1.47	30	15	32	25,470	2,094
15	Pd-DEBP4	9,400	4,300	2.19	13	6	4	2,720	2,096
16	Pd-DEBP6	12,000	5,200	2.31	17	7	6	4,140	2,096
17	Pd-DEBP20	26,000	17,000	1.53	36	23	20	14,100	2,096

[a] Weight average molecular weight.
[b] Number average molecular weight.
[c] Molecular weight distribution M_w/M_n.
[d] Number of repeating units calculated from M_w.
[e] Number of repeating units calculated from M_n.
[f] Number of repeating units calculated from ^{31}P NMR data referred to internal and terminal phosphine moieties.

Reactions of trans-*[Pd(PBu$_3$)$_2$Cl$_2$] with DEBP*

Pd-containing polymetallaynes are less studied materials, and a few papers are found[46–48] in the literature probably because of their relative lower stability with respect to Pt-containing polymers.

In our case, reactions analogous to those reported for Pt-DEBP polymers were first carried out in the presence of 5% CuI for the synthesis of Pd-containing materials. The final products showed elemental analyses nonconsistent with the proposed structure, probably due to an impurity containing the Cu byproduct. Attempts to purify this crude Pd-polymer by chromatography or crystallization resulted unsuccessful, probably due to intermolecular charge transfer of the alkynyl ligand from Pd(II) site to Cu(I) according to a literature report.[43] When the polymerization reactions of Pd(II) were performed in the absence of CuI, the expected Pd-DEBP polymer was obtained. ^{31}P NMR spectra showed peaks at $\delta = 10.56$ and 11.30 ppm attributed to terminal and internal Pd units, respectively, in analogy with literature data.[48] The variation of the reaction time allowed us to isolate different oligomers, from four units (4 h) up to about 20 units (8 h) (Table 1). Attempts to increase the molecular weight by increasing the temperature (up to 60 °C) or the reaction time in the range of 24–48 h were unsuccessful, yielding oligomers with short chains (about six repeating units), probably due to decomposition of the growing chain.

Infrared and GPC Molecular Weight Characterization

IR spectroscopy was used as a completion for the characterization of the polymers. The stretching mode ν C≡C, found in our materials at about 2100 cm^{-1}, seems to be almost unaffected by the chain length. However, looking at Table 2, where the GPC molecular weights and infrared stretching mode of the C≡C moiety are reported, most of the samples with M_w in the range of 3800–42,000 g°mol^{-1} and M_n in the range of 2500–10,000 g°mol^{-1} show an IR band at about 2096 cm^{-1}, that is interpreted as an increase of moderate entity in the π-conjugation through the alkyne moieties with respect to platinum(II) acetylides with low σ-donor strength phosphines[49] and in comparison with the binuclear complex[17] *trans*, *trans*-[ClPt(PBu$_3$)$_2$(—C≡C—C$_6$H$_4$—C$_6$H$_4$—C≡C—Pt(PBu$_3$)$_2$Cl], where the stretching mode was found at 2113 cm^{-1}.

The molecular weights determined with GPC have to be considered with some caution in the case of rigid-rod polymers, because of the

calibration procedure performed with polysterene standards, whose random coil structure leads to hydrodynamic properties quite different from those of rigid rods and usually is reported as an overestimation of the actual molecular weight.

Thermal Analysis

TGA and differential thermal analyses (DTA) were carried out on the organometallic polymers to investigate the range of stability in air of the polymetallaynes. The precursor monomer (2) was also investigated as a comparison. The TG and DTA curves of DEBP (2) show that, at the decomposition temperature (T = 152 °C), an exothermic explosive reaction occurs with a weight loss of about 50%. The total combustion occurs at higher temperature, and a total weight loss is achieved at about 600 °C. The TG and DTA curves of **14**, Pt-DEBP32, indicate that the polymer is stable until about T = 280 ± 3 °C. The weight loss (20%) occurs with exothermic reaction at T = 285 °C, probably due to the loss of the organic spacer DEBP (theoretical loss 25%) and further loss happens at T = 360 °C (weight loss 49%) were correlated to phosphines release (theoretical loss 50%). Over 605 °C an exothermic broad peak occurs, because of carbon residues. The final residue of 31% can be interpreted as residues due to Pt and PtO. The TG and DTA curves of **17**, Pd-DEBP20, show a lower thermal stability in comparison with Pt-DEBP32; in fact, the Pd polymer is stable up to 150 °C and after this temperature a first loss of weight (30%) occurs, with an exothermic peak due to the DEBP moiety loss (theoretical value 28%), and a second exothermic peak at 306 °C, with weight loss 53% due to the release and combustion of PBu_3 units (theoretical 57%). The total combustion leaves about 17% of material, probably due to the transition metal oxide PdO. These experimental data are in agreement with the expected behavior of Pd-containing polymers compared with those containing Pt; a higher stability is achieved when DEBP is bonded between two Pt atoms in the polymer chain. Both polymers reveal no discernible glass transitions in the DSC curves.

Optical Characterization

An attempt of understanding the evolution of the polymerization reactions was performed by UV–vis measurements run every 15 min from the beginning to the end. Already after the first

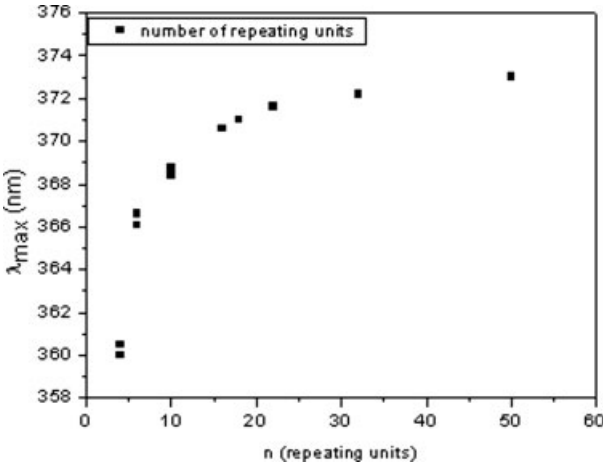

Figure 5. UV absorption maxima versus number of repeating units in the polymetallaynes.

15 min, the λ_{ass} (maximum absorption wavelength) absorption peak of the precursor complex (λ_{ass} = 262 nm for the cis isomer) disappeared, and a broadband formed by the overlapping of the absorption of the complex with that of DEBP (λ_{ass} = 290 nm) was found together with a peak of low intensity at 340 nm due to low-molecular-weight oligomers (Fig. 5). Upon increasing the reaction time, a decrease of the intensity of the broadband and increase of the absorption at higher wavelengths, corresponding to the presence of longer oligomers (Table 3), was detected till at the end of the polymerization only the absorption at λ_{ass} = 360–375 nm is observed. This trend is reproduced for all the reactions, either using the *cis* or the *trans* precursor $[Pt(PBu_3)_2Cl_2]$, suggesting the fast isomerization of the cis isomer, thus leading to linear oligomers and polymers with trans configuration around the Pt center.

The correlation between chain length of oligomers and polymers (determined from ^{31}P NMR spectra and GPC measurements, respectively) and UV–vis absorption maxima has been investigated and the data are reported in Figure 6. A smooth redshift of this peak toward longer wavelengths in the range 358–375 nm is observed for oligomers with a number of repeating units 4, 6, and 50, because of π–π^* transitions of the organic moiety and associated to the first singlet excited state extending through the macromolecule. These values of optical absorption are fairly in agreement with the findings reported in the literature for a series of Pt(II) and Hg(II) polymetallaynes and dinuclear model complexes.[12] A sharp increase of the molecular

Table 3. Photophysical Data: Absorption and Emission Maxima, Quantum Yield η, band gap E_g for Pt-DEBP and Pd-DEBP Polymetallaynes (Spectra Collected at Room Temperature in $CHCl_3$)

Compound	λ_{ass}[a] (nm)	ε_0[b] (10^3 L g^{-1} cm^{-1})	λ_{emis}[c] (nm)	$\lambda_{emis} - \lambda_{ass}$ (nm)	η (%)	E_g[d] (eV)
6 Pt-DEBP4	304.0sh, 360.0	69.97	396.0	36.0	0.24	3.24
7 Pt-DEBP6	302.6sh, 368.0	81.47	398.1	30.1	0.34	3.19
8 Pt-DEBP50	303.8sh, 373.2	88.00	399.0	25.8	0.27	3.17
9 Pt-DEBP4	304.0sh, 360.0	76.49	396.0	36.0	0.24	3.25
10 Pt-DEBP10	365.2	77.87	399.2	34.2	0.26	3.20
14 Pt-DEBP32	373.0	88.06	400.3	27.3	0.26	3.17
17 Pd-DEBP20	343.2	70.51	464.9; 488.4	121.7; 145.7	4.07	3.24

[a] Maximum absorption wavelength.
[b] Extinction coefficient.
[c] Maximum emission wavelength.
[d] Optical band gap.

weight (roughly 50 repeating units, i.e. M_w = 40,000) does not induce further electronic delocalization, being the absorption maximum at 373 nm, that is about the same value found for platinum polymetallaynes with substituted 1,4-diethynylbenzene spacers.[15] In analogy with similar polymetallaynes,[50] a moderate electronic delocalization extending through the conjugated chain, including the metal chromophore, is detected. However, the effect of the conjugation length on the optical redshift is effective only for oligomers with 4–20 Pt-containing units.

The emission spectra, at room temperature, of oligomers **6** Pt-DEBP4, **7** Pt-DEBP6, **10** Pt-DEBP10, and **8** Pt-DEBP50 polymer show λ_{emis} (maximum emission wavelength) values in the range of 400–430 nm (green-blue region, emission from the S_1 state, intraligand fluorescence) with a progressive small shift to lower energies by increasing the chain length and a related increase of the quantum yield (Table 3).

Looking at the shape of the spectra in Figure 6(b), a shoulder at higher wavelength (for example at about 425 nm, main band at 400 nm) is detected, which is assigned to emission from the triplet state T_1 (phosphorescence), according to literature reports.[51]

The optical absorption maxima of Pd-DEBP polymer is found in a narrow range at λ_{ass} = 343 nm (Table 3) and the emission spectra of **17**, Pd-DEBP20, show a main band at λ_{emis} = 464.9 nm with a shoulder at λ_{emis} = 488.4 nm. It is interesting that, in the case of **17**, Pd-DEBP20 (Fig. 7), the quantum efficiency in the luminescence spectra, recorded at the same concentration of the solutions of Pt-DEBP samples,

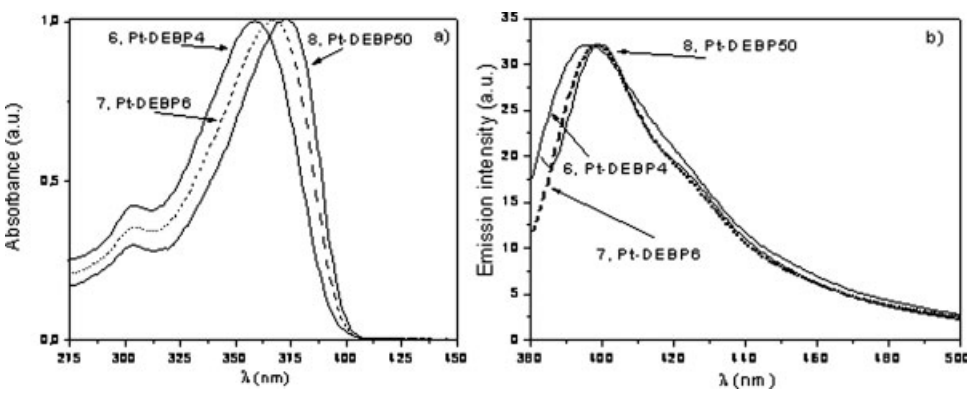

Figure 6. Room temperature optical absorption (a) and photoluminescence spectra (b) in $CHCl_3$ for Pt-DEBP based oligomers 4, 7, and polymer 8.

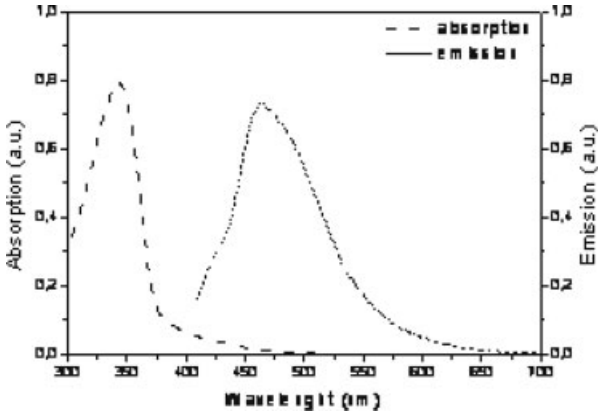

Figure 7. Room temperature optical absorption and photoluminescence spectra in $CHCl_3$ for 17, Pd-DEBP20 polymer.

is higher by a factor of 10 and that there is a separation between the absorption and luminescence maxima of 121.7 nm.

In our study, the aromatic monomer–metal complex is designed to include a linking group that could partially disrupt the conjugation, because of the mutual rotation of the phenyls in DEBP spacer. The diethynylbiphenyl at the solid state shows the two phenyl rings bent at 43° out of the plane.[52] This lack of planarity is almost totally reduced when binuclear Pd and Pt alkynyl complexes are formed,[17] so that the effective conjugation length remains and can be likewise extended to the case of oligomers and polymers.

Investigation of the Electronic Structure by XPS Studies

The chemical and electronic structure of polymers and oligomers was further studied by XPS, with the aim of finding a relationship between chain length and optical or electronic properties.

Table 4. XPS Data: BE, FWHM, and Atomic Ratios for Pt-DEBP Polymer and Oligomers

Compound	Signal	BE[a] (eV)	FWHM[b] (eV)	*n*/Pt experimental[c]	*n*/Pt Theoretical[d]
1 *cis*-$Pt(PBu_3)_2Cl_2$	C1s	285.00; 283.72	1.45; 1.45	23.00	24
	$Pt4f_{7/2}$	73.03	1.55	1	1
	$P2p_{3/2}$	131.21	1.46	1.99	2
	$Cl2p_{3/2}$	198.06	1.2	1.70	2
3 *trans*-$Pt(PBu_3)_2Cl_2$	C1s	285.00; 283.60	1.41; 1.41	22.98	24
	$Pt4f_{7/2}$	72.97	1.55	1	1
	$P2p_{3/2}$	131.35	1.54	1.98	2
	$Cl2p_{3/2}$	198.09	1.36	1.90	2
6 Pt-DEBP4	C1s	285.00; 283.64	1.60; 1.60	44.02	36
	$Pt4f_{7/2}$	72.82	1.77	1	1
	$P2p_{3/2}$	131.23	1.65	2.45	2
	$Cl2p_{3/2}$	198.30	1.83	0.52	0.50
7 Pt-DEBP6	C1s	285.00; 283.32	1.87; 1.82	38.2	32
	$Pt4f_{7/2}$	72.40	2.02	1	1
	$P2p_{3/2}$	131.28	2.07	2.12	2
	$Cl2p_{3/2}$	198.10	2.02	0.39	0.28
8 Pt-DEBP50	C1s	285.00; 283.43	1.60; 1.60	40.75	39.77
	$Pt4f_{7/2}$	72.86	1.72	1	1
	$P2p_{3/2}$	131.26	1.45	2.11	2
	$Cl2p_{3/2}$	198.17	1.83	0.19	0.03
10 Pt-DEBP10	C1s	285.00; 283.59	1.83; 1.83	40.23	38.40
	$Pt4f_{7/2}$	72.84	2.00	1	1
	$P2p_{3/2}$	131.28	1.84	2.22	2
	$Cl2p_{3/2}$	198.22	2.16	0.26	0.20
14 Pt-DEBP32	C1s	285.00; 283.30	1.76; 1.76	45.73	39.46
	$Pt4f_{7/2}$	72.79	1.77	1	1
	$P2p_{3/2}$	131.19	1.58	1.88	2
	$Cl2p_{3/2}$	198.03	1.83	0.32	0.06

[a] Binding energy.
[b] Full width at half-maximum.
[c] Number of atoms versus Pt atom.

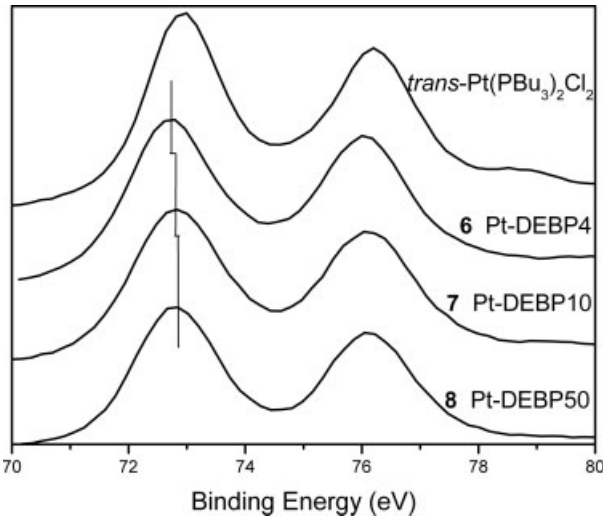

Figure 8. XPS spectra: Pt4f core level versus chain length of Pt-DEBP oligomers and polymer.

To this purpose, the XPS spectra of precursor cis and trans complexes were compared with the spectra of samples with increasing number of repeating units. Moreover, the stability of the Pd-DEBP polymer, a material particularly sensitive to the environment although with interesting optical properties, over a period of time as long as 2 years was investigated.

Electronic Structure of Pt-DEBP Samples

A systematic investigation of Pt-DEBP polymer and oligomers has been performed acquiring the C1s, Pt4f, P2p, Cl2p core level spectra, and the data are collected in Table 4, where the core level BE and full width at half-maximum are reported.

The C1s, P2p, Cl2p BE values of samples prepared from cis and trans precursors are quite close, showing that the same configuration around the metal was obtained, regardless the configuration of the precursor complex, which is hardly detectable with these measurements.

The trans configuration of the oligomers and polymers could be assessed unambiguously from NMR studies. However, XPS spectra evidenced a shift of the Pt4f BE toward lower values by increasing the number of repeating units of the samples (Fig. 8); this behavior was already observed for Pt-containing rigid-rod organometallic complexes and oligomers,[15] suggesting a conjugation and electronic delocalization through the orbitals of the dialkynyl spacer and of the transition metal. The low BE shoulder in the C1s spectrum at about 283 eV was attributed to carbons bonded to the metal atoms.[53] On the basis of theoretical studies on the band structure of organometallic polymetallaynes,[54] 6p and 5d orbitals of the metal are involved in the electronic communication along the linear chain giving rise to an increase of the electron density around the metal, thus decreasing the positive charge and the BE value upon increasing the number of conjugated repeating units in the macromolecule. These data confirm the optical results reported in the previous paragraph.

Table 5. XPS Data: BE, FWHM, and Atomic Ratios for 17, Pd-DEBP20

Compound	Signal	BE[a] (eV)	FWHM[b] (eV)	*n*/Pd Experimental[c]	%Pd(0)	*n*/Pd Theoretical[c]
17, Pd-DEBP20	C1s	285.00; 283.27	2.01; 2.01	54.72		40
(fresh)	Pd3d5/2	335.48; 337.51	2.00; 2.00	1	16	1
	P2p3/2	131.00	2.01	3.47		2
	Cl2p3/2	197.91	1.98	1		_
17, Pd-DEBP20	C1s	285.00; 283.30	2.01; 2.01	41.53		40
(3 months aged)	Pd3d5/2	336.10; 337.85	2.00; 2.00	1	26	1
	P2p3/2	131.07	2.01	2.45		2
	Cl2p3/2	198.20	2.02	0.57		_
17, Pd-DEBP20	C1s	285.00; 283.10	1.97; 1.97	44.32		40
(3 years aged)	Pd3d5/2	335.50; 338.11	1.80; 1.80	1	27	1
	P2p3/2	130.62	2.00	2.73		2
	Cl2p3/2	198.70	2.01	0.46		_

[a] Binding energy.
[b] Full width at half-maximum.
[c] Number of atoms versus Pd atom.

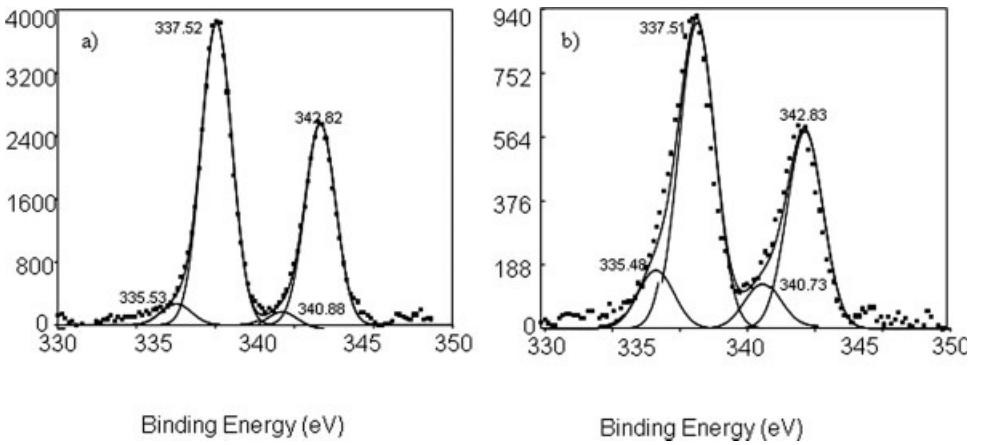

Figure 9. XPS spectra Pd3d peak fit results: (a) fresh polymer; (b) Three months aged sample.

The evaluation of atomic ratios (Table 4) allows to define the chain length that is found in good agreement with the elemental analysis and GPC measurements. The number of chlorine atoms, that may be due to terminal ending groups in short oligomers, is overestimated for some samples because of the clustering of the purification solvent $CHCl_3$. XPS measurements, performed after aging the samples several months, have established the environmental stability of Pt-containing polymers.

Electronic Structure and Stability of Pd-DEBP Samples

Beside the higher reactivity of Pd complexes in comparison with Pt ones, the difficulty of studying Pd-DEBP samples arose also from their low solubility, which affected the formation of thin films, and from their sensitivity to temperature (ambient) and aging. The stability–instability of Pd-DEBP materials was in fact observed by means of XPS measurements performed on polymeric samples. In Table 5, the C1s, Pd4f, P2p, Cl2p core level values are collected for a freshly prepared and purified polymer and for the same sample aged for 3 months and 3 years; the atomic ratios are nearly consistent with the chemical structure of Pd-DEBP, showing that the amount of Pd(0) is about 6% for the fresh polymer and that Pd(0) content is enhanced to 15% after aging for 3 months. The reduction of palladium is detected from the peak fit analysis of the Pd3d XPS spectra, which show two couples of signals (each couple is due to the spin-orbit components of Pd3d, $3d_{5/2}$, and $3d_{3/2}$, respectively), with the $Pd3d_{5/2}$ peaks at 337.51 eV and 335.48 eV BE attributed to Pd(II) and Pd(0), respectively (Fig. 9). Analogous behavior of Pd sites was observed in Pd(II) ethynylthiophene complexes and oligomers upon interaction with chromium,[55] where the reduction of Pd was induced by the interface formation. XPS investigations on samples of Pd-DEBP aged 1, 2, and 3 years have shown that after 1 year the Pd(0) content is about 16%, reaching the value of 27% after 2 and 3 years. These results indicate that a moderate stability of Pd-containing polymers is attainable in a few weeks and that after this time a degradation of samples occurs.

Scanning Electron Microscopy

The nanostructured surface morphology of polymetallaynes can modify the properties of these materials, in particular, their performance in sensor devices.[4,15] To investigate more suitable

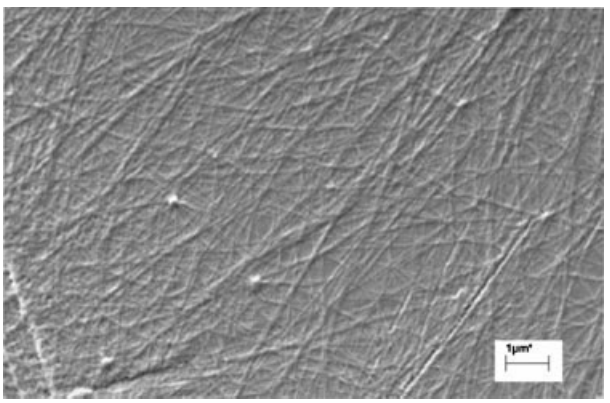

Figure 10. SEM image for 8, Pt-DEBP50, film obtained by casting from toluene solution on gold substrate.

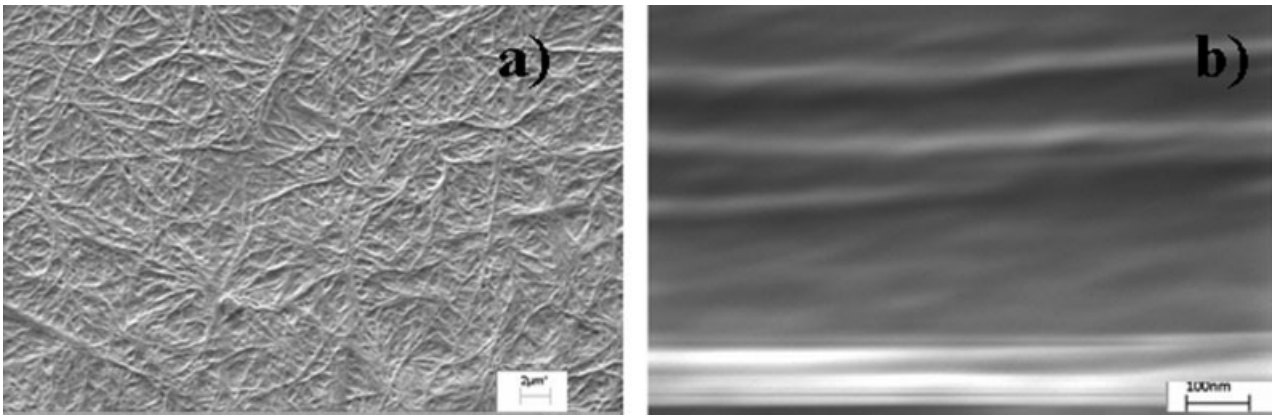

Figure 11. SEM images for 17, Pd-DEBP20, films obtained by casting from toluene solution on gold substrate (a) and border detail (b).

modes for the achievement of nanostructured features, SEM measurements were performed on films of Pt-DEBP and Pd-DEBP and the formation of molecular self-assembling was detected.

SEM images of a Pt-DEBP film, obtained by casting the polymer from a $CHCl_3$ solution onto different substrates, revealed the fibrous nature of aggregates, consistent with an alignment of the polymeric chains.

Many factors affect the growth and the morphology of the nanostructures. For example, the control of the evaporation rate of the polymeric solution, performed by choosing solvents with selected vapor pressure, can lead to the formation of well-defined wires. In Figure 10 as an example the SEM image of **8**, Pt-DEBP50 polymer, deposited on gold substrate from toluene solution, is reported showing fibrils with diameter in the range of 50–100 nm randomly oriented.

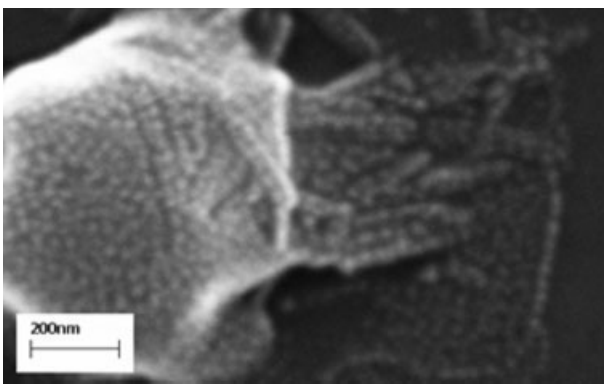

Figure 12. SEM image for 17, Pd-DEBP20, film obtained by casting from $CHCl_3$ solution on gold substrate.

In the case of **17**, Pd-DEBP20 polymer, similar fibril morphology was observed by casting toluene solutions on gold substrate [Fig. 11(a)]. The fibrils showed an average length of microns with diameters of tens of nanometers. The analysis of the morphological feature seen in detail on the border of the substrate revealed a more ordered formation of polymer nanofibrils [Fig. 11(b)], suggesting an influence also of the film thickness on the assembling of the polymer chains.

When **17**, Pd-DEBP20, was deposited on a glass substrate from $CHCl_3$ solution, the nucleation points can be observed (Fig. 12), from which rows of the polymeric nanoparticles appeared structured by linear aggregation of nanospheres (diameter 20–30 nm), which are believed to be the precursors of the fibrils.

CONCLUSIONS

The reactivity of 4,4′diethynylbiphenyl with *cis* and *trans* $[MCl_2(PBu_3)_2]$, with M = Pt or Pd, for the synthesis of oligomers, with defined chain length, and polymers has been studied with careful check of the reaction conditions. The formation of oligomers with a number of repeating units in the range 4–10 can be promoted by avoiding the use of the catalyst CuI. Each oligomer can be separated by column chromatography and characterized. This result is a promising prerequisite for the achievement of molecular wires with desired length at the nano/microscale. All the synthesized materials have a linear molecular structure with the metal centers in trans configuration. The optical absorp-

tion and emission of the macromolecules can be finely tuned, depending on the number of repeating units of the oligomers. Pd-containing polymers exhibit higher luminescence properties than the Pt-containing ones, although they are less stable. Both Pt-DEBP and Pd-DEBP show the property of assembling in nanostructured fibrils by simple casting from their solutions onto Au or other substrates, thus suggesting their use in nanotech applications. Nanofibers with diameter in the range 50–100 nm were obtained controlling the deposition conditions.

The financial support to this research by MIUR (Italy), projects FIRB n° RBAU01Y7BX_001 and COFIN 2004 n° 2004031237 are gratefully acknowledged.

REFERENCES AND NOTES

1. Kingsborough, R. P.; Swager, T. M. In Progress in Inorganic Chemistry; Karlin, K. D., Ed.; Wiley: New York, 1999; Vol. 48, pp 123.
2. Nguyen, P.; Gomez-Elipe, P.; Manners, I. Chem Rev 1999, 99, 1515.
3. Kohler, A.; Wilson, J. S.; Friend, R. H.; Al-Suti, M. K.; Gerhard A.; Bassler H. J Chem Phys 2002, 116, 9457.
4. Wong, W. Y. Coord Chem Rev 2005, 249, 971.
5. Liu, L.; Wong, W.-Y.; Shi, J.-X.; Cheah, K.-W. J Polym Sci A: Polym Chem 2006, 44, 5588.
6. Wang, F.; Lai, Y. H.; Han, M. Y. Org Lett 2003, 5, 4791.
7. Manners, I. Synthetic Metal containing polymers; Wiley VCH, 2004, 208.
8. Hagihara, N.; Sonogashira, K.; Takahashi, S. Adv Polym Sci 1981, 41, 149.
9. Younus, M.; Köhler, A.; Cron, S.; Chawdhury, N.; Al-Mandhary, M. R. A.; Khan, M. S.; Lewis, J.; Raithby, P. R. Angew Chem Int Ed Engl 1998, 37, 3036.
10. Chow, H.-F.; Leung, C.-F.; Xi, L.; Lau, L. W. M. Macromolecules 2004, 37, 3595.
11. Siemens, P.; Gubler, U.; Bosshard, C.; Günter, P.; Diederich, F. Chem—Eur J 2001, 7, 1333.
12. Wong, W.-Y.; Lu, G.-L.; Choi, K.-H.; Shi, J.-X. Macromolecules 2002, 35, 3506.
13. Liu, L.; Wong, W.-Y.; Poon, S.-Y.; Shi, J.-X.; Cheah, K.-W.; Lin, Z. Chem Mater 2006, 18, 1369.
14. Zhou, G.-J.; Wong, W.-Y.; Cui, D.; Ye, C. Chem Mater 2005, 17, 5209.
15. Marsen, B.; Sattler, K. Phys Rev B 1999, 60, 11593.
16. Fratoddi, I.; Battocchio, C.; Polzonetti, G.; Mataloni, P.; Russo, M. V.; Furlani, A. J Organomet Chem 2003, 674, 10.
17. Russo, M. V.; Lo Sterzo, C.; Franceschini, P.; Biagini, G.; Furlani, A. J Organomet Chem 2001, 619, 49.
18. Battocchio, C.; D'Acapito, F.; Fratoddi, I.; La Groia, A.; Polzonetti, G.; Roviello, G.; Russo, M. V. Chem Phys 2006, 328, 269.
19. Bolasco, A.; Cimenti, F.; Frezza, A.; Furlani, A.; Infante, G.; Muraglia, E.; Ortaggi, G.; Polzonetti, G.; Russo, M. V.; Sleiter, G. Polymer 1992, 33, 3049.
20. Caliendo, C.; Verona, E.; D'Amico, A.; Furlani, A.; Infante, G.; Russo, M. V. Sens Actuators B 1995, 24/25, 670.
21. Penza, M.; Cassano, G.; Sergi, A.; Lo Sterzo, C.; Russo, M. V. Sens Actuators B 2001, 81, 88.
22. Long, N. J.; Wong. C. K.; White, A. J. P. Organometallics 2006, 25, 2525.
23. Iucci, G.; Infante, G.; Polzonetti, G. Polymer 2002, 43, 655.
24. Liu, L.; Poon, S. Y.; Wong, W.-Y. J Organomet Chem 2005, 690, 5036.
25. Fratoddi, I.; Altamura, P.; Lo Sterzo, C.; Furlani, A.; Galassi, E.; D'Amico, A.; Russo, M. V. Polym Adv Technol 2002, 13, 269.
26. Caliendo, C.; Fratoddi, I.; Russo, M. V. Appl Phys Lett 2002, 80, 4849.
27. Caliendo, C.; Fratoddi, I.; Lo Sterzo, C.; Russo, M. V. J Appl Phys 2003, 93, 10071.
28. Russo, M. V.; Infante, G.; Polzonetti, G.; Contini, G.; Tourillon, G.; Parent, Ph.; Laffon, C. J Electron Spectrosc Relat Phenom 1997, 85, 53.
29. D'Acapito, F.; Fratoddi, I.; D'Amato, R.; Russo, M. V.; Contini, G.; Davoli, I.; Mobilio, S.; Polzonetti, G. Sens Actuators B 2004, 100, 131.
30. Tour, J. M.; Jones, L. R., II; Pearson, D. L.; Lamba, J. J. S.; Burgin, T. P.; Whitesides, G. M.; Allara, D. L.; Parikh, A. N.; Atre, S. V. J Am Chem Soc 1995, 117, 9529.
31. Zehner, R. W.; Sita, L. R. Langmuir 1997, 13, 2973.
32. Oleynik, I. I.; Kozhushner, M. A.; Posvyanskii, V. S.; Yu, L. Phys Rev Lett 2006, 96, 096803.
33. Joachim, C.; Gimzewski, J. K.; Aviram A. Nature 2000, 408, 541.
34. Carroll, R. L.; Gorman, C. B. Angew Chem Int Ed Engl 2002, 41, 4378.
35. Svelto, O. Principles of Lasers; Plenum: New York, 1989; p 6.
36. Beamson, G.; Briggs, D. High Resolution XPS of Organic Polymers, the Scienta ESCA300 Database; Wiley: New York, 1992.
37. Scofield, J. M. J Electron Spectrosc Relat Phenom 1976, 8, 129.
38. Takahashi, S.; Kuroyama, Y.; Sonogashira, K.; Hagihara, N. Synthesis 1980, 627.
39. Kauffman, G. B.; Teter, L. A. Inorg Synth 1963, 7, 245.
40. Zhang, L.; Niu, Y.-H.; Jen, A. K.-Y.; Lin, W. Chem Commun 2005, 1002.

41. Hurtley, F. R. Organomet Chem Rev A 1979, 6, 119.
42. Sonogashira, K. J Organomet Chem 2002, 653, 46.
43. Osakada, K.; Sakata, R.; Yamamoto, Y. Organometallics 1997, 16, 5354.
44. Bruce, M. I.; Davy, J.; Hall, B. C.; Jansen van Galen, Y.; Skelton, B. W.; White, A. H. Appl Organomet Chem 2002, 16, 559.
45. Harvey, J. N.; Heslop, K. M.; Guy Orpen, A.; Pringle, P. G. Chem Commun 2003, 278.
46. Takahashi, S.; Onitsuka, K.; Takei, F. Macromol Symp 2000, 156, 69.
47. Yang, M.; Li, Y.; Hiller, M. J Mater Sci Lett 2003, 22, 707.
48. La Groia, A.; Ricci, A.; Bassetti, M.; Masi, D.; Bianchini, C.; Lo Sterzo, C. J Organomet Chem 2003, 683, 406.
49. Schull, T. L.; Kushmerick, J. G.; Patterson, C. H.; Gorge, C.; Moore, M. H.; Pollak, S. K.; Shashidhar, R. J Am Chem Soc 2003, 125, 3202.
50. Khan, M. S.; Al-Mandhary, M. R. A.; Al-Suti, M. K.; Corcoran, T. C.; Al-Mahrooqi, Y.; Attfield, J. P.; Fieder, N.; David, W. F.; Shankland, K.; Friend, R. H.; Köhler, A.; Marseglia, E. A.; Tedesco, E.; Tang, C. C.; Raithby, P. R.; Collings, J. C.; Roscoe, K. P.; Batsanov, A. S.; Stimson, L. M.; Marder, T. B. New J Chem 2003, 27, 140.
51. Chawdhury, N.; Köhler, A.; Friend, R. H.; Wong, W. Y.; Lewis, J.; Younus, M.; Raithby, P. R.; Corcoran, T. C.; Al-Mandhary, M. R. A.; Khan, M. S. J Chem Phys 1999, 110, 4963.
52. Ogata, Y.; Nakajima, K. Tetrahedron 1964, 20, 43.
53. Polzonetti, G.; Iucci, G.; Russo, M. V.; Paolucci, G.; Cocco, D.; Capellini, G. Chem Phys Lett 1998, 292, 515.
54. Springborg, M. J Solid State Chem 2003, 176, 311.
55. Iucci, G.; Polzonetti, G.; Altamura, P.; Paolucci, G.; Goldoni, A.; Russo, M. V. J Vac Sci Technol A 2000, 18, 248.